

## Land Cover Changes Based on Landsat Imagery Interpretation

Chairiyah Umi Rahayu<sup>1</sup>, Indarto Indarto<sup>1✉</sup>, Alfian Wiji Pradiksa<sup>1</sup>, Bayu Taruna Wijaya Putra<sup>1</sup>,  
Rufiani Nadzirah<sup>1</sup>

<sup>1</sup>Department of Agricultural Engineering, Jember University, Jember, INDONESIA.

### Article History :

Received : 5 June 2022  
Received in revised form : 30 September 2022  
Accepted : 16 November 2022

### Keywords :

Soil erosion,  
RUSLE model,  
GIS,  
Serayu watershed,  
Vegetation cover

### ABSTRACT

*This paper presents the use of satellite data (i.e., Landsat-5 & Landsat-8) to interpret the change of land cover from 1997 to 2020. The study area covered the administrative boundary of Lumajang Regency. The land-cover map of the year 1997 was derived from Landsat-5. The Land-cover map of the year 2020 was interpreted from Landsat-8. This study uses two methods of image classifications (i.e., unsupervised and supervised). The procedure includes image enhancement, registration, and classification. The supervised classification produces 7 classes of Land cover (i.e., forest, pavement/urban area), paddy field, plantation, rural area, water body and sand mining area. Unsupervised classification produced four 5 class i.e., forest, built-area, paddy field, rural area, and plantation. Supervised classification done the overall and kappa accuracy = 86% and 82%, while unsupervised classification = 73% and 64% for 1997 imagery. Furthermore, for 2020 image, the Supervised classification reaches the overall and kappa accuracy = 93% and 90%, while unsupervised classification done 81% and 72%. The supervised classification method gives a better result than unsupervised. Comparison of 1997 to 2020, it also shows the increase in pavement or build-area, followed by paddy field, rural area, and sand-mining. The change also appears as the decrease in forest and plantation areas.*

✉Corresponding Author:  
indarto.ftp@unej.ac.id

## 1. INTRODUCTION

Information on changes in land cover can be obtained by manual digitization, but this requires a lot of time, effort and money. Remote sensing can be used to analyze changes in land cover or allotment effectively and efficiently (Indarto 2017). Furthermore, land cover (LC) and land use (LU) refer to the EUROSTAT publication (2001) as follows: "land cover (LC) states a physical description of a space on the earth's surface and with this description allows various bio-physical categories to be distinguished. Observation of land cover can be done through various methods, including: direct observation (human eye),

aerial photography and satellite sensors. Meanwhile, land use (LU) refers to the functional dimension of the description of the area related to economic purposes (eg: area for residential), industrial or commercial purposes, for agriculture or forests, for recreation or nature conservation (EUROSTAT 2001).

LCLU thematic maps can be generated from existing conventional maps or derived from satellite imagery. Both types of maps can be used to study the LCLU and its changes, as in research conducted by (Eremiášová and Skokanová 2009) and (Ptak and Ławniczak 2012). Furthermore, Lambin et al. (2001); Martínez & Mollicone (2012); Efroymsen et al. (2016); dan Song et al. (2018) provide an example of how to further explore the causal relationship between changes in the LCLU and its consequences for society and the environment. In other cases, several studies have tried to integrate various kinds of image data through image fusion techniques to study the LCLU phenomenon more comprehensively (Moran, 2010; Li et al., 2012; Wężyk et al., 2016; Tavares et al., 2019).

Landsat-5 was launched on March 1, 1984, operating in a polar orbit and carrying a TM (Thematic Mapper) sensor which has a spatial resolution of 30 x 30 m in bands 1, 2, 3, 4, 5 and 7. The TM sensor observes objects in the earth's surface with 7 spectral bands. Channels (bands) 1, 2 and 3 are visible light. Furthermore, channels 4, 5 and 7 contain near infrared (NIR) rays, medium infrared, and band 6 is thermal infrared (TIR) which has a spatial accuracy of 120 x 120 m (Table 1). Coverage area of one (1) scene image = 175 x 185 km on the surface of the earth. Landsat 5 has the ability to cover the same area on the earth's surface every 16 days at an orbital altitude of 705 km (EOS 2020).

Landsat-8 imagery has 2 sensors, namely OLI (Operational Land Imager) and TIRS (Thermal Infrared Sensor) sensors. The total channels on Landsat 8 are 11 channels. Eight channels have a spatial accuracy of 30 m (channels 1 to 7 and channel 9). The new ultra-blue channel is positioned as channel-1 (band-1), useful for coastal and aerosol studies. Channel-9 has also recently been used to identify cirrus clouds. The spatial accuracy of panchromatic channel-8 (band-8) is 15 m. Thermal channels no.10 and 11 (band-10 and band-11) are useful for identifying surface temperatures with an accuracy of 100 m. The size of 1 Landsat 8 scene is 170 km north-south and 183 km east-west or (106 mi x 114 mi). TIRS channels (bands 10 and 11) were obtained with an accuracy of 100 m but resampled to 30 m in the final product sent to consumers (Indarto, 2017; EOS, 2020). Band name, wavelength and resolution for each band on Landsat-8 can be seen in Table 2.

**Table 1.** Spatial and spectral accuracy of the Landsat-5 channel

Band	Band Name	Wavelength (µm)	Resolution (m)
1	Visible Blue	0,45 - 0,52	30
2	Visible Green	0,52 - 0,60	30
3	Visible Red	0,63 - 0,69	30
4	NIR	0,76 - 0,90	30
5	SWIR 1	1,55 - 1,75	30
6	Thermal	10,40 - 12,50	120
7	SWIR 2	2,08 - 2,35	30

Source : (EOS 2020)

**Table 2.** Landsat-8 band characteristics

Band	Nama Band	Spectral accuracy ( $\mu\text{m}$ )	Spatial accuracy (m)
1	Coastal	0,43 - 0,45	30
2	Blue	0,45 - 0,51	30
3	Green	0,53 - 0,59	30
4	Red	0,63 - 0,67	30
5	NIR	0,85 - 0,88	30
6	SWIR 1	1,57 - 1,65	30
7	SWIR 2	2,11 - 2,29	30
8	Pan	0,50 - 0,68	15
9	Cirrus	1,36 - 1,38	30
10	TIRS 1	10,60 - 11,19	100
11	TIRS 2	11,50 - 12,51	100

Source : (Indarto, 2017).

Mapping using satellite imagery in principle is classifying pixels into a group of pixels based on a certain logic, so that objects or features that exist in nature can be described as similar as possible. This can be done by various methods, for example: classification, segmentation, matching-learning or other algorithms. The calcification method is very commonly used. [Khorram et al. \(2013\)](#) stated that most image classification methods are based on "hard-logic", using both spectral information and temporal-spatial patterns. This "hard-logic" based classification is generally divided into two, namely supervised and unsupervised classification.

Guided classification is a classification method that is preceded by a sampling process (training area) for each land cover category based on survey results (ground check) ([Schowengerdt, 2007](#)). In contrast, the unsupervised classification method or better known as the clustering method is a classification that is carried out without any training areas in each land cover category ([Campbell & Wynne, 2011](#)). The classification algorithm will determine the distance between pixels and estimate cluster centers according to the initial criteria provided by the user. The user only defines the required criteria. Therefore unsupervised classification can be said to be a natural classification process, because it is only based on the value that exists for each pixel in the image itself ([Indarto, 2017](#)). The accuracy of the classification results can be measured by various methods. The most common method used to measure the accuracy of the classification results is the confusion matrix ([Foody 2004](#)). The concept of an error matrix has generally been written up in textbooks on remote sensing ([Lillesand et al., 2008](#); [Campbell & Wynne, 2011](#)).

Data on changes in land use can be obtained by manual digitization, but this is time consuming and need a lot effort and money. Therefore, technology is needed to determine changes in land use effectively and efficiently. The technology is remote sensing. Remote sensing is a technology/technique for measuring or obtaining information about an object or feature on the earth's surface without having direct contact with the object being measured ([Indarto, 2017](#)). One of the data that can be used for remote sensing is satellite imagery. There are various types of satellite imagery, from low resolution to high resolution. Satellite imagery can be accessed for free or not. One example of unpaid satellite imagery with moderate resolution is

Landsat satellite imagery. In addition to knowing the magnitude of changes in land use in Lumajang Regency, this research was also conducted to determine the optimum performance.

## 2. MATERIALS AND METHODS

### 2.1. Study location and data input

The research area covers the entire area of Lumajang district. A total of 843 ground control points (GCP) are used to assist the guided classification process (Figure 1). The GCP is obtained from the results of digitization using GPS which are scattered in the research area. Furthermore, the creation of the training area is carried out by creating a polygon with GCP reference, Table 3 displays the training area data including the number, area and training area statistics per land use class.

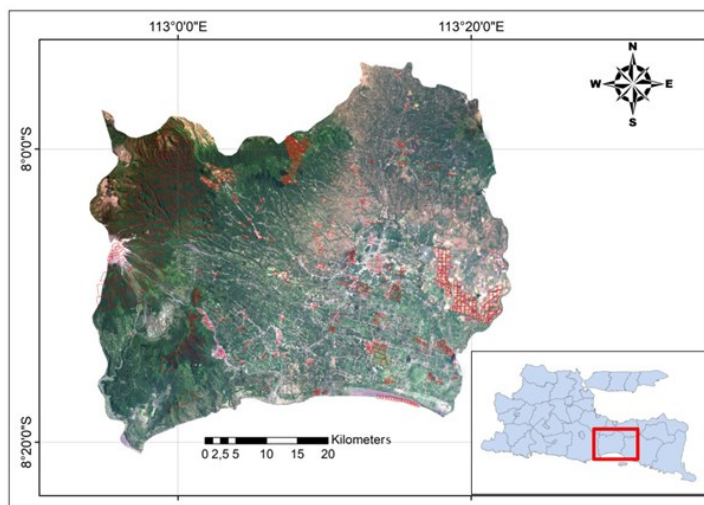


**Figure 1.** Study Locations and training area locations

The equipment used in the study consisted of: GPS, SAGA GIS software, and a camera. SAGA GIS version 6 was obtained from the SAGA official website (Conrad et al. 2015). Data analysis was carried out at FTP, University of Jember. The main inputs in this study include: landsat-5 imagery, landsat-8 imagery, Google earth, and RBI maps. The downloaded Landsat data are Landsat-5 data recorded on 14 June 1997 and Landsat 8 data recorded on 28 September 2020 (Table 4). The data is obtained by downloading on the website (USGS 2019).

**Table 3.** Training Area Data

Class	Number of Training Area	Total Area (Ha)	Least Area (Ha)	Highest Area (Ha)	Median (Ha)
Pavement/	150	1.119,49	1,20	35,20	6,90
Forest	150	15.716,90	3,70	381,00	81,60
Paddy	150	2.831,20	1,40	72,00	13,20
Plantation	150	3.983,70	2,80	72,00	25,35
Dry land	140	2.633,90	1,10	66,90	17,60
Sand area	100	1.622,40	2,80	42,10	16,20
Water body	3	77,90	12,20	36,00	29,70
<b>Total</b>	<b>843</b>	<b>27.985,49</b>			

**Table 4.** Image metadata

Date Acquired	Path / Rows	Cloud Cover (%)	Land Cloud Cover (%)	Data Type	Orbit	Sun Elevation (°)	Sun Azimuth (°)	Angle
14 June 1997	118/66	9	3	L1TP /T1	Ascending	42.57	46.94	Nadir
07 Oct 2020	118/66	3.5	1.1	L1TP /T1	Ascending	63.34	76.87	Nadir

## 2.2. Research Procedures

The research procedure includes: composite band blinding, image cropping (clips), image correction, image enhancement, image classification (unsupervised and supervised), accuracy testing, and interpretation of changes in land use or land cover from 1997 to 2020 (Figure 2).

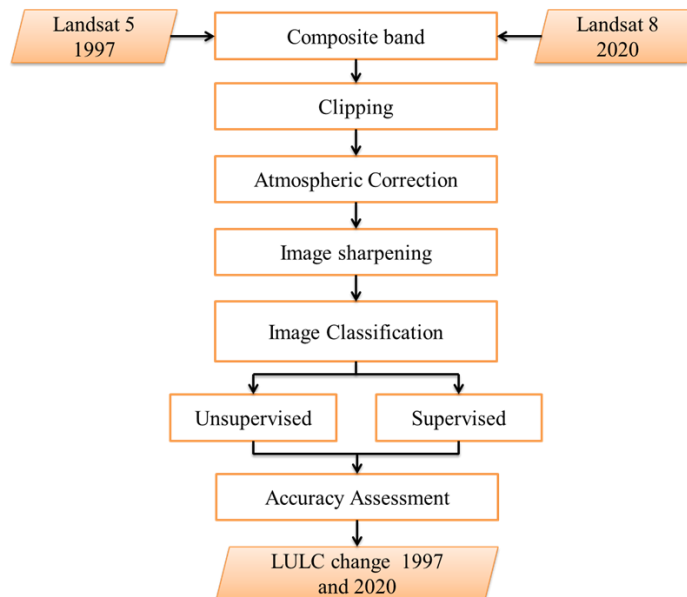


**Figure 2.** Flow chart of research procedure

### 2.2.1. Composite Bands

Composite bands are performed to combine several bands into one layer. In the SAGA GIS application it is referred to as a grid. Composite bands aim to simplify interpretation and distinguish class one from the others based on the spectral value generated from the composite. Composite bands use a combination of bands 6, 5 and 4 as the RGB bands on Landsat-8. Whereas on Landsat-5, the combination used is bands 5, 4 and 3. The band combination was chosen because it can display colors according to the original appearance on the earth's surface (natural color) (Figure 3).

### 2.2.2. Image Cropping

Image cropping serves to limit the research area and reduce the size of the image file. The area of Lumajang Regency is in part of the image scan, so to obtain appropriate data, image cropping is done based on the boundaries of the area to be studied. The

composite bands are then cut using the clip with polygon menu. The polygon boundary layer for the Lumajang Regency area (\*.shp format) is used for cutting.

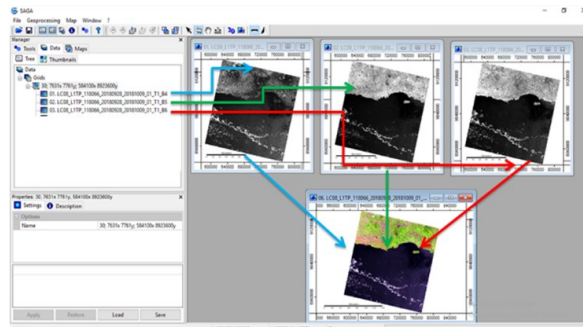


Figure 3. Composite band illustration

### 2.2.3. Atmospheric and geometric correction of the image

Atmospheric correction cleans image data from disturbances in the atmosphere, such as clouds. Atmospheric correction can remove clouds covering the image, but not all clouds can be removed. The only clouds that can be removed are thin clouds, while thick clouds cannot be removed. The geometric correction corrects the image to the earth's coordinate system, so that the image information corresponds to the actual location on the earth. Atmospheric corrections were made for all bands and using the Geographic coordinate system WGS 84.

### 2.2.4. Improved image appearance

Image enhancement to improve image quality visually so that images are easy to interpret. Appearance in the image between one feature (object) and other features can be easily distinguished. The process of visual interpretation of a digital image that has improved quality is in principle a series of operations that can simplify and integrate (synchronize) things that can be seen and thought by the human eye with computer manipulation capabilities (Indarto, 2017). Image sharpening using 8-panchromatic channels (pansharpening) in SAGA GIS.

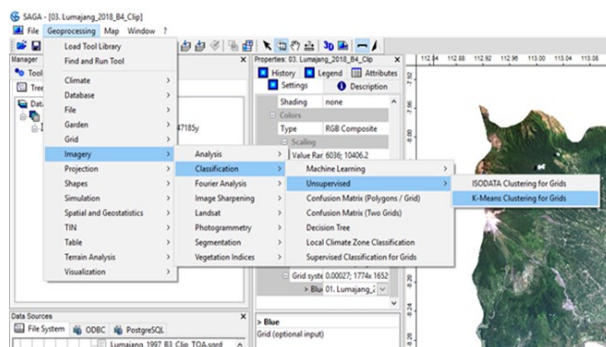


Figure 4. Unsupervised classification

### 2.2.5. Unsupervised classification

The commands performed on SAGA are Geoprocessing – imagery – classification – unsupervised - k-means (Figure 4). The classification process produces 20 initial clusters. Then the 20 clusters were reclassified into 5 classes consisting of: (1) forests,

(2) urban area, (3) paddy fields, (4) plantation and (5) dry land. The process of reclassification (reclass) is carried out to combine several of the same classes into one class.

### 2.2.6 Supervised classification

The supervised method uses the maximum likelihood algorithm, using the the Geoprocessing – imagery – classification – supervised menu for clustering grids as depicted in Figure 5.

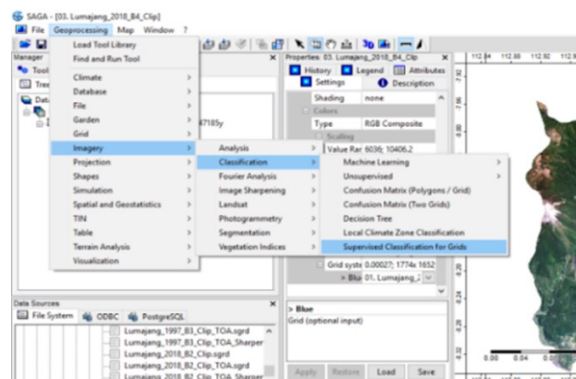


Figure 5. Classification of supervised

Supervised classification uses 843 training area data. The training area is made based on the GCP obtained from direct surveys in the field and via Google Earth. The training area is used as a reference for determining classes in the classification process. Based on the 843 training areas, then reclassification was carried out into 7 classes, namely: (1) forests, (2) urban area, (3) paddy fields, (4) plantation, (5) dry lands, (6) water bodies and (7) sand area. After 7 classes are formed, the next step is to change the color of the class produced by the classification process according to the RBI (Rupa Bumi Indonesia) map.

### 2.2.7 Accuracy Test

The accuracy test of the classification results is carried out to determine the level of accuracy of the map results produced through a digital image classification process. The accuracy test method used is the confusion matrix to determine the accuracy value of Kappa and Overall. The higher the accuracy test value, the more accurate the resulting map will be. The overall accuracy value is obtained based on the percentage of the number of pixels that are classified correctly divided by the total number of pixels. The recommended accuracy test is using Kappa because it takes into account all parts in the error matrix while Overall only takes into account pixels that are correctly classified (Jaya, 2010, Sampurno dan Thoriq, 2016). According to the National Institute of Aeronautics and Space (LAPAN) the acceptable accuracy value is above 75% (LAPAN, 2014). Meanwhile, according to the United States Geological Survey (USGS 2019) the acceptable accuracy test value is above 85%.

## 3. RESULTS AND DISCUSSION

Classification using the supervised method is able to distinguish seven (7) classes,:( 1) forests, (2) settlements/urban area, (3) paddy field, (4) plantation, (5) dry land, (6) water bodies, and (7) sand-mining area. Classification using the unsupervised method

was only able to produce five (5) land use classes, i.e: forest, settlements/urban area, paddy field, plantation and dry lands.

### 3.1 Visual comparison of composite bands

Figure 5a shows the Landsat-5 image with band 3,2,1 composite. Figure 5b shows the Landsat-8 image with band 4,3,2 composite. The two images display the image as it appears to our eyes.

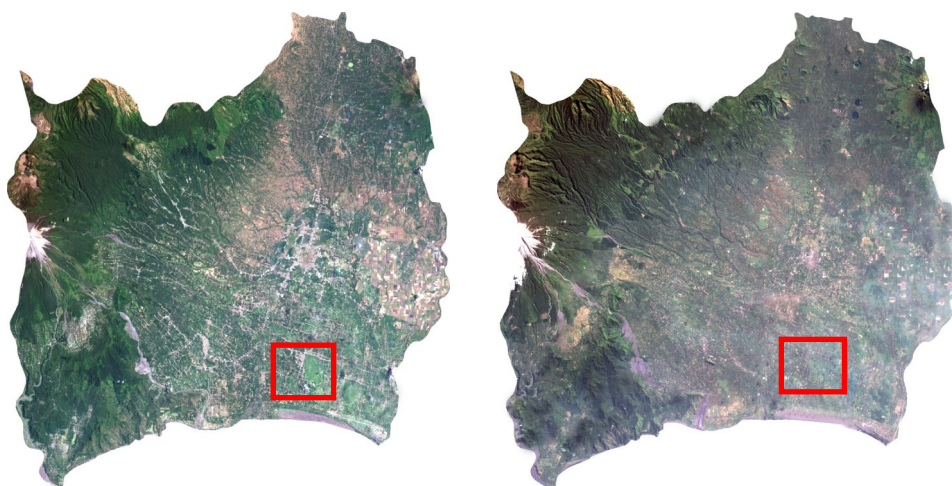


**Figure 6.** Composite comparison of Landsat 5 and Landsat 8 image bands: Composite band 3,2,1 from Landsat-5 imagery in 1997 (left), and Composite bands 4,3,2 of the Landsat-8 imagery in 2020 (right)

### 3.2. Classification of Landsat-5 Imagery Vs. RBI Digital

Figure 7 displays a zoom visualization of the classification results compared to the RBI map for the area sampled in the red rectangle in Figure 6. The area within the red rectangular polygon is 45 km<sup>2</sup>. In this study the 1997 Landsat-5 imagery is more similar than the RBI map, considering that the RBI maps were made between 1999 and 2001. So that the land use features may not differ much between the two. In Landsat 8 imagery, as a comparison, we used manually digitized thematic maps from Google Earth images for 2020. So digitizing Google Earth images covering an area of 45 km<sup>2</sup> is used as a control to compare the quality of the classification results.

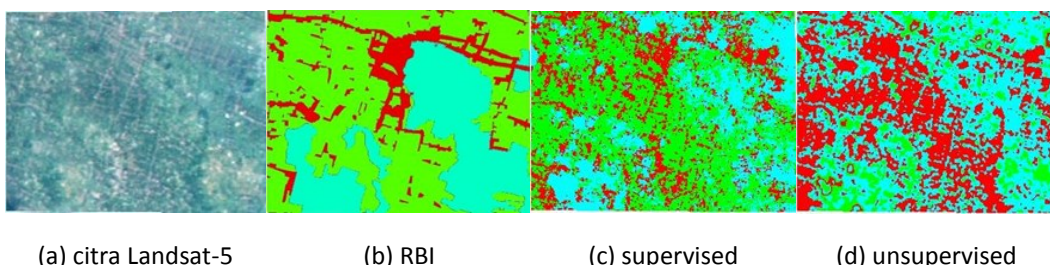


**Figure 7.** Details of the 1997 image classification

Classification results are also assessed with overall and kappa accuracy. The results of Landsat-5 image classification (unspervised and supervised methods) were

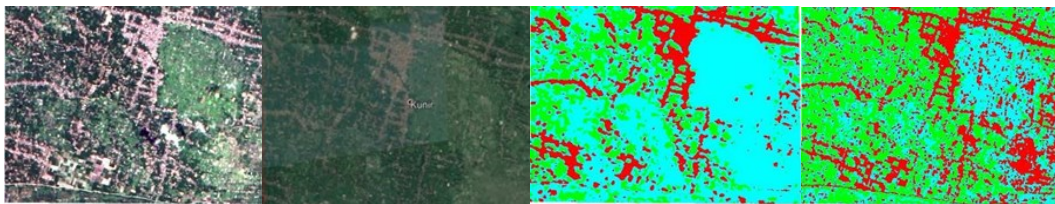
compared with the RBI map (Table 5). In this case, the OA (overall accuracy) and KA (kappa accuracy) in Table 5 are calculated only for the 45 km<sup>2</sup> area.

**Table 5.** Comparison of classification result

No	method	Pavement/ Urban area		Paddy field		Plantation		Accuracy	
		km <sup>2</sup>	%	km <sup>2</sup>	%	km <sup>2</sup>	%	OA	KA
1	RBI	4,3	9,9	16,4	36,4	24,3	53,7		
2	Unsupervised	13,3	29,5	16,5	35,6	15,9	34,9	55 %	49 %
3	Supervised	5	11,1	16,1	35,7	23,9	53,2	77 %	58 %

### 3.3. Comparison of Classification Landsat-8 Imagery Vs. Google Earth

Figure 8 visually displays the results of the classification of Landsat-8 imagery using the supervised and unsupervised methods, compared to the manual digitization. Digitization is based on the 2020 Google Earth image. The results of Landsat-5 image classification (unspervised and supervised methods) were compared with the Google Earth (Table 5)



(a) Landsat-8 image      (b) Google Earth      (c) supervised      (d) unsupervised

**Figure 8.** Landsat-8 vs. Google Earth classification results for 2020

**Table 6.** Comparison of classification results with Google Earth

No	Appearance	Pavement/ Urban area		Paddy field		Plantation		Accuracy (%)	
		km <sup>2</sup>	%	km <sup>2</sup>	%	km <sup>2</sup>	%	OA	KA
1	Google Earth	5.5	12.5	28.4	62.2	11.1	25.3		
2	Unsupervised	12.6	28	16.5	36.6	15.9	35.4	89	83
3	Supervised	5.9	13.2	27.3	60.4	11.8	26.4	100	100

This comparison (Figure 7 and Figure 8) yields three classes of land cover, namely: settlements, paddy fields and gardens. The results of the accuracy test on a sample covering an area of 45 km<sup>2</sup> show that the comparison of Landsat-8 with Google Earth has better accuracy than the comparison of Landsat-5 with RBI. This is because the RBI map used as a comparison was produced around 2001, while the Landsat-5 data used was 1997. In contrast to the comparison between Landsat-8 and Google Earth, it used the same year, namely 2020. The results of the supervised classification method are close to those of manual digitization. , on the other hand, the unsupervised method differs greatly. Table 7 shows a comparison of the overall and kappa accuracy calculated for all areas mapped using the guided and unsupervised classifications, for both 1997 and 2020. In general, the guided classification is better.

**Table 7.** Results of classification accuracy

Indicator	Supervised		Unsupervised	
	1997	2020	1997	2020
Overall Accuracy	83%	88%	68%	76%
Kappa Accuracy	80%	86%	62%	72%

**Table 8.** Land use change 1997 to 2020

Class	Area			
	km <sup>2</sup>		%	
	1997	2020	1997	2020
Pavement / Urban area	25,92	49,56	1,45	2,77
Forest	581,13	605,14	32,47	33,81
Paddy fields	492,06	356,73	27,49	19,93
plantation	413,83	380,76	23,12	21,27
Dry land	236,52	322,13	13,21	18
Sand-mining area	28,36	57,63	1,58	3,22
Water body	0,72	0,71	0,04	0,04
Unclassified (Cloud cover)	11,46	17,9	0,64	1

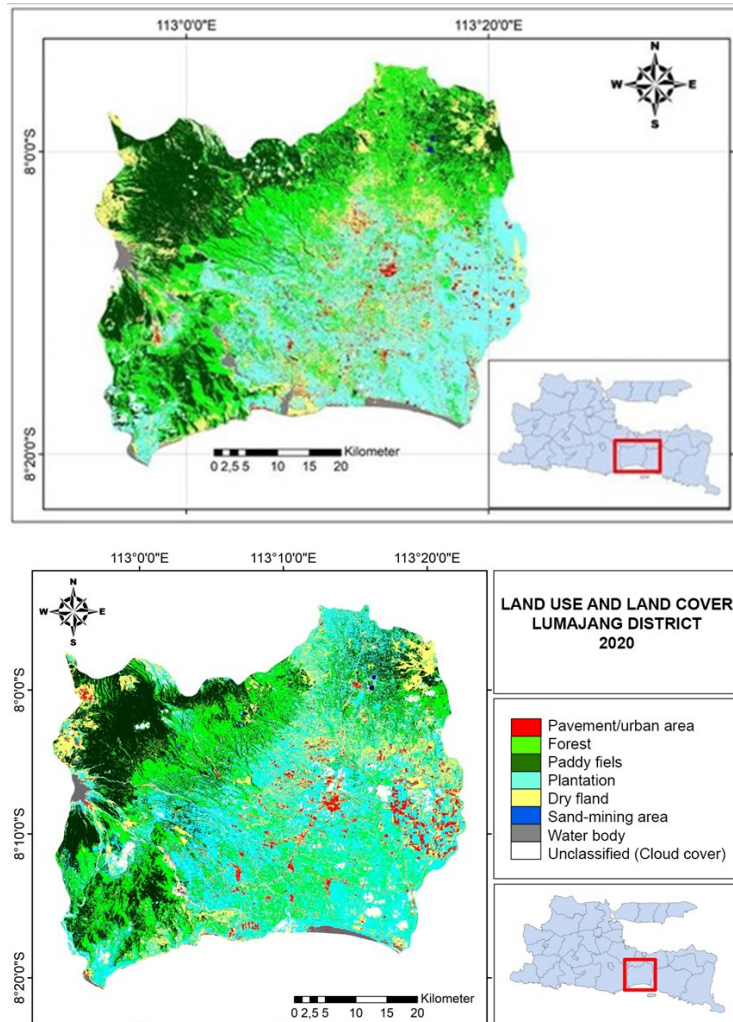
### 3.4. Analysis of Land Use Changes from 1997 to 2020

Table 8 shows a comparison of each land use class in km<sup>2</sup> and the percentage per total area (%) for 1997 and 2020 based on supervised classification. The table shows an increasing residential area, this is due to population growth which continues to increase every year, so the need for housing is also increasing. Paddy fields and fields also increased. This can be caused by an error in the classification results. Errors in classification can be caused by: the spatial resolution of the images used, the heterogeneity of the study area, the training samples that do not represent each type of land cover, and the topography of the study area. For example, we often find mixed landscape patches in the middle extensive rice fields. This mixed area can consist of housing and house yards, annual vegetation (not forest areas or plantations), and seasonal plants. Therefore, using 10m x 10m sentinel pixels, these mixed landscape patches are difficult to classify (Lu et al. 2004). Furthermore, Figure 9 displays the results of the guided classification for Landsat-5 (1997) and Figure 10 displays the results of the Guided Classification of Landsat-8 (2020)

## 4. CONCLUSION

The supervised classification method produces better accuracy than the unsupervised method. Based on the guided classification, it is known that land use in Lumajang district has changed from 1997 to 2020. Settlements experienced an increase in area of ±23.64 km<sup>2</sup>; paddy fields experienced an increase in area of ±24.01 km<sup>2</sup>; forests have decreased in area of ±135.33 km<sup>2</sup>; gardens experienced a decrease in area of ±33.07 km<sup>2</sup>; dry fields experienced an increase in area of ±85.61 km<sup>2</sup>; the sand fields area increased by ±29.27 km<sup>2</sup> and the water body decreased by ±0.01 km<sup>2</sup>. Research has demonstrated how Landsat imagery can be used to detect and calculate land use or cover changes in district areas. However, there are still errors in the classification

results caused by the spatial resolution of the images used, the heterogeneity of the study area, the training samples that do not represent each type of land cover, and the topography of the study area.



**Figure 9.** Land use map for 1997 (upper) and for 2020 (bottom)

## REFERENCES

- Campbell, J.B., & Wynne, R.H. (2011). *Introduction to Remote Sensing*. Fifth edition. Guilford Publications.
- Conrad, O., Bechtel, B., Bock, M., Dietrich, H., Fischer, E., Gerlitz, L., Wehberg, J., Wichmann, V., & Böner, J. (2015). System for automated geoscientific analyses (SAGA) v. 2.1.4. *Geosci. Model Dev.*, *8*(7), 1991–2007. <https://doi.org/10.5194/gmd-8-1991-2015>
- Efroymson, R.A., Kline, K.L., Angelsen, A., Verburg, P.H., Dale, V.H., Langeveld, J.W.A., & McBride, A. (2016). A causal analysis framework for land-use change and the potential role of bioenergy policy. *Land Use Policy*, *59*, 516–527. <https://doi.org/10.1016/j.landusepol.2016.09.009>
- EOS. (2020). Landsat 5 (TM) Information, Bands, Operational Data and More. Retrieved June 25, 2020, from <https://eos.com/landsat-5-tm/>

- Eremiášová, R., & Skokanová, H. (2009). Land use changes (recorded in old maps) and delimitation of the most stable areas from the perspective of land use in the Kašperské Hory Region. *Journal of Landscape Ecology*, **2**(1), 20–34. <https://doi.org/https://doi.org/10.2478/v10285-012-0012-5>
- EUROSTAT. (2001). *Manual of Concepts on Land Cover and Land Use Information Systems*. Retrieved from <http://europa.eu.int>
- Foody, G.M. (2004). Thematic map comparison: Evaluating the statistical significance of differences in classification accuracy. In *Photogrammetric Engineering and Remote Sensing*. American Society for Photogrammetry and Remote Sensing. <https://doi.org/10.14358/PERS.70.5.627>
- Indarto, I. (2017). *Pengindraan Jauh : Metode Analisis & Interpretasi Citra Satelit*. Yogyakarta: Penerbit Andi.
- Jaya, I. (2010). *Analisis Citra Digital: Perspektif Penginderaan Jauh Untuk Pengelolaan Sumber Daya Alam*. Bandung: IPB Press.
- Khorram, S., Nelson, S.A.C., Cakir, H., & van der Wiele, C.F. (2013). Digital image acquisition: Preprocessing and data reduction. In *Handbook of Satellite Applications*. Editors: J.N. Pelton, S. Madry, & S. Camacho-Lara. New York: Springer, 809–837. [https://doi.org/10.1007/978-1-4419-7671-0\\_46](https://doi.org/10.1007/978-1-4419-7671-0_46)
- Lambin, E.F., Turner, B.L., Geist, H.J., Agbola, S.B., Angelsen, A., Bruce, J. W., Coomes, O.T., Dirzo, R., Fischer, G., Folke, C., George, P.S., Homewood, C., Imbernon, J., Leemans, R., Li, X., Moran, E.F., Mortimore, M., Ramakrishnan, P.S., Richards, J.F., Skånes, H., & Xu, J. (2001). The causes of land-use and land-cover change: Moving beyond the myths. *Global Environmental Change*. Elsevier Ltd. [https://doi.org/10.1016/S0959-3780\(01\)00007-3](https://doi.org/10.1016/S0959-3780(01)00007-3)
- LAPAN (Lembaga Penerbangan dan Antariksa Nasional). (2014). Penyusunan Pedoman Pengolahan Digital Klasifikasi Penutup Lahan Menggunakan Penginderaan Jauh. Jakarta, 1–25.
- Li, G., Lu, D., Moran, E., Dutra, L., & Batistella, M. (2012). A comparative analysis of ALOS PALSAR L-band and RADARSAT-2 C-band data for land-cover classification in a tropical moist region. *ISPRS Journal of Photogrammetry and Remote Sensing*, **70**, 26–38. <https://doi.org/10.1016/j.isprsjprs.2012.03.010>
- Lillesand, T.M., Kiefer, R.W., & Chipman, J.W. (2008). *Remote Sensing and Image Interpretation* (6<sup>th</sup> ed.). New Jersey.
- Lu, D., Mausel, P., Moran, E., & Rudy, J. (2004). Comparison of land-cover classification methods in the Brazilian Amazon basin. *Photogrammetric Engineering and Remote Sensing*, **70**(6), 723–731. <https://doi.org/10.14358/PERS.70.6.723>
- Martínez, S., & Mollicone, D. (2012). From land cover to land use: A methodology to assess land use from remote sensing data. *Remote Sensing*, **4**(4), 1024–1045. <https://doi.org/10.3390/rs4041024>
- Moran, E.F. (2010). Land cover classification in a complex urban-rural landscape with quickbird imagery. *Photogrammetric Engineering and Remote Sensing*, **76**(10), 1159–1168. <https://doi.org/10.14358/PERS.76.10.1159>
- Ptak, M., & Ławniczak, A.E. (2012). Changes in land use in the buffer zone of lake of the Mała Wełna catchment. *Limnological Review*, **12**(1), 35–44. <https://doi.org/https://doi.org/10.2478/v10194-011-0043-z>
- Sampurno, R.M. & Thoriq, A. (2016). Klasifikasi tutupan lahan menggunakan citra landsat 8 operational land imager (OLI) di Kabupaten Sumedang. *Jurnal Teknotan*. **10**(2), 61–70.
- Schowengerdt, R.A. (2007). Chapter 9 - Thematic classification. In *Remote Sensing: Models and*

- Methods for Image Processing*. Burlington: Academic Press, 387-456. <https://doi.org/10.1016/B978-012369407-2/50012-7>
- Song, X.P., Hansen, M.C., Stehman, S.V., Potapov, P.V., Tyukavina, A., Vermote, E.F., & Townshend, J.R. (2018). Global land change from 1982 to 2016. *Nature*, **560**(7720), 639–643. <https://doi.org/10.1038/s41586-018-0411-9>
- Tavares, P.A., Beltrão, N.E.S., Guimarães, U.S., & Teodoro, A.C. (2019). Integration of sentinel-1 and sentinel-2 for classification and LULC mapping in the urban area of Belém, eastern Brazilian Amazon. *Sensors*, **19**(5), 1140. <https://doi.org/10.3390/s19051140>
- USGS. (2019). *Landsat 8 (L8) Data Users Handbook Version 4.0*. Department of the Interior, U.S. Geological Survey. Retrieved from [https://prd-wret.s3-us-west-2.amazonaws.com/assets/palladium/production/atoms/files/LSDS-1574\\_L8\\_Data\\_Users\\_Handbook\\_v4.0.pdf](https://prd-wret.s3-us-west-2.amazonaws.com/assets/palladium/production/atoms/files/LSDS-1574_L8_Data_Users_Handbook_v4.0.pdf)
- Wężyk, P., Hawryło, P., Szostak, M., Pierzchalski, M., & Kok, R.De. (2016). Using geobia and data fusion approach for land use and land cover mapping. *Quaestiones Geographicae*, **35**(1), 93–104. <https://doi.org/https://doi.org/10.1515/quageo-2016-0009>